

A wearable noncontact free-rotating hybrid nanogenerator for self-powered electronics

Dongjie Jiang^{1,3} | Han Ouyang² | Bojing Shi² | Yang Zou^{1,3} | Puchuan Tan² |
Xuecheng Qu^{1,3} | Shengyu Chao^{1,3} | Yuan Xi¹ | Chaochao Zhao^{1,4} |
Yubo Fan² | Zhou Li^{1,3} 

¹CAS Center for Excellence in Nanoscience, Beijing Key Laboratory of Micro-nano Energy and Sensor, Beijing Institute of Nanoenergy and Nanosystems, Chinese Academy of Sciences, Beijing, China

²Beijing Advanced Innovation Centre for Biomedical Engineering, Key Laboratory for Biomechanics and Mechanobiology of Ministry of Education, School of Biological Science and Medical Engineering, Beihang University, Beijing, China

³School of Nanoscience and Technology, University of Chinese Academy of Sciences, Beijing, China

⁴Department of Biomedical Engineering, School of Medical Engineering, Foshan University, Foshan, China

Correspondence

Yubo Fan, School of Biological Science and Medical Engineering, Beihang University, Beijing 100083, China.
Email: yubofan@buaa.edu.cn

Zhou Li, Beijing Institute of Nanoenergy and Nanosystems, Chinese Academy of Sciences, Beijing, 100083, China.
Email: zli@binn.cas.cn

Funding information

China Postdoctoral Science Foundation, Grant/Award Number: 2019M660410; National Key R&D Project from Minister of Science and Technology, China, Grant/Award Numbers: 2016YFA0202703, 2016YFC1102202; National Natural Science Foundation of China, Grant/Award Numbers: 11421202, 21801019, 61875015, 81971770; National Postdoctoral Program for Innovative Talent, Grant/Award Number: BX20190026; Natural Science Foundation of Beijing Municipality, Grant/Award Number: 7204275; The 111 Project, Grant/Award Number: B13003; National Youth Talent Support Program

Abstract

Self-powerability is a new trend in the development of portable devices. Harvesting biomechanical energy to power personal information electronics is of great significance. In this work, we report a wearable noncontact free-rotating hybrid nanogenerator (WRG), which is constituted by a triboelectric nanogenerator and an electromagnetic generator. A continuous output over 2 seconds can be achieved during one instantaneous incentive by external force, which is improved by two orders of magnitude compared to other wearable nanogenerators due to its unique mechanical energy storage design. The WRG can be integrated into shoes to generate an output energy of 14.68 mJ in each stepping, which meets the power requirements of most personal information electronics. The wireless sensor, GPS, and smartphone can be powered by the WRG continuously. The WRG is expected to be applied in self-powered information electronics extensively in the future.

KEYWORDS

electromagnetic generator, hybrid nanogenerator, self-powered electronics, triboelectric nanogenerator, wearable electronics

Dongjie Jiang, Han Ouyang, and Bojing Shi contributed equally to this work.

This is an open access article under the terms of the Creative Commons Attribution License, which permits use, distribution and reproduction in any medium, provided the original work is properly cited.

© 2020 The Authors. *InfoMat* published by John Wiley & Sons Australia, Ltd on behalf of UESTC.

1 | INTRODUCTION

With the advent of the information age, individuals are relying on electronic devices for information sensing, communication, and computing.¹⁻³ These applications utilize battery-powered devices whose batteries have a limited useful life.^{4,5} Powering billions of these distributed devices is a huge challenge.^{6,7} Up to now, the limited capacity of power source has impeded the service life and performance of wearable/portable information electronics.^{8,9} It is an emergency to develop both efficient and stable wearable energy harvesting technologies.^{10,11} Fortunately, energy harvesting technologies and devices have demonstrated the unique capabilities in powering information electronics, such as nanogenerators, electromagnetic generators (EMGs), and biofuel cells.¹²⁻¹⁶

As a new type of renewable, sustainable energy technology, nanogenerator has been reported comprehensively since 2006.^{17,18} This technology can convert mechanical energy into electrical power based on triboelectric or piezoelectric effects.¹⁹⁻²³ Some studies have integrated the triboelectric nanogenerator (TENG) into commercial shoes to harvest biomechanical energy from human motions to light up LEDs in real time.²⁴⁻²⁶ Besides, the nanogenerators based on piezoelectric and electromagnetic induction effects also have been utilized to powering wearable information electronics.^{8,21,27,28} These energy harvesting technologies show an encouraging prospect in mobile applications.²⁹⁻³³ However, the biomechanics motion is always discontinuous and of low frequency.³⁴ For the existing wearable nanogenerator, each biomechanical motion can produce tens of milliseconds of effective output only. It is difficult to keep the energy harvester scavenge biomechanical energy effectively and power for information electronics continuously. The rotating disk-based TENGs can generate a continuous high-frequency output, which provides an opportunity to drive electronics continuously.^{35,36}

Mechanical energy storage technology has been widely used in hydraulic and wind power generation to increase the effective output time.^{37,38} The gravitational potential energy of water is stored by the dam and released slowly to achieve continuous and efficient power generation. Here, we demonstrated a wearable non-contact free-rotating hybrid nanogenerator (WRG), as a mobile power source based on mechanical energy storage technology. The WRG also named “wind-fire wheel nanogenerator,” which was inspired by Chinese myths of Nezha. The WRG can convert the noncontinuous gravitational potential energy of humans into the continuous rotational kinetic energy of the rotor by a unique mechanical transmission structure. An instantaneous incentive by external force can generate a continuous

electrical output over 2 seconds. The effective output time is improved by two orders of magnitude compared to other wearable nanogenerators. The WRG can generate 14.68 mJ energy during one stepping, which meets the power requirements of most mobile information electronics. In addition, the WRG has been achieved in powering the wireless sensor, GPS, and smartphone continuously and stably, which is expected to be applied to self-powered information electronics in the future.

2 | RESULTS AND DISCUSSION

As schematically illustrated in Figure 1A, the structure of the WRG mainly consists of two parts: the hybrid nanogenerator and the wearable gravitational potential energy storage portion. The hybrid nanogenerator is made up of a noncontact free-rotating TENG and an EMG. By utilizing the laser cutting technology, two circular acrylic disks with a diameter of 60 mm and a thickness of 5 mm are fabricated to be the substrate. Six magnets have been held in the acrylic disk with an alternating magnetic manner as the rotor, and the corresponding six coils are held in another acrylic disk as the stator. In the meantime, a piece of polytetrafluoroethylene (PTFE) film (~300 μm in thickness) is tailored into a six-segment structure and role as the tribo-charged layer, which is attached onto the rotor. Two separated aluminum sheets with complementary six-segment shapes (~500 μm in thickness and 6 cm in diameter) are attached onto the stator as stationary metal electrodes (Figure 1A, B). To increase the triboelectric charge density during the electrification process, we fabricate the micropattern structure on the tribo-charged layer and metal electrodes.^{39,40} The inductively coupled plasma (ICP) process is utilized to carve nanorods on the surface of the PTFE film by reactive ion etching (Figure 1D).

The wearable gravitational potential energy storage portion is manufactured through 3D printing and laser cutting techniques (Figure S1). Due to the unique mechanical transmission structure, the WRG can convert the human body's gravitational potential energy into the rotational kinetic energy of the rotor. When the human body gravity loads on the WRG, the foot will press the pedal down to push the rack forward. Through a series of gear transmission structure, the rotatable acrylic disk will keep turning in a clockwise direction even if the rack moves backward. Therefore, the rotor can be accelerated continuously and reach a maximum rotating speed of 13.74 rps during human motion. The noncontinuous human body's gravitational potential energy is transformed into the continuous rotational kinetic energy of

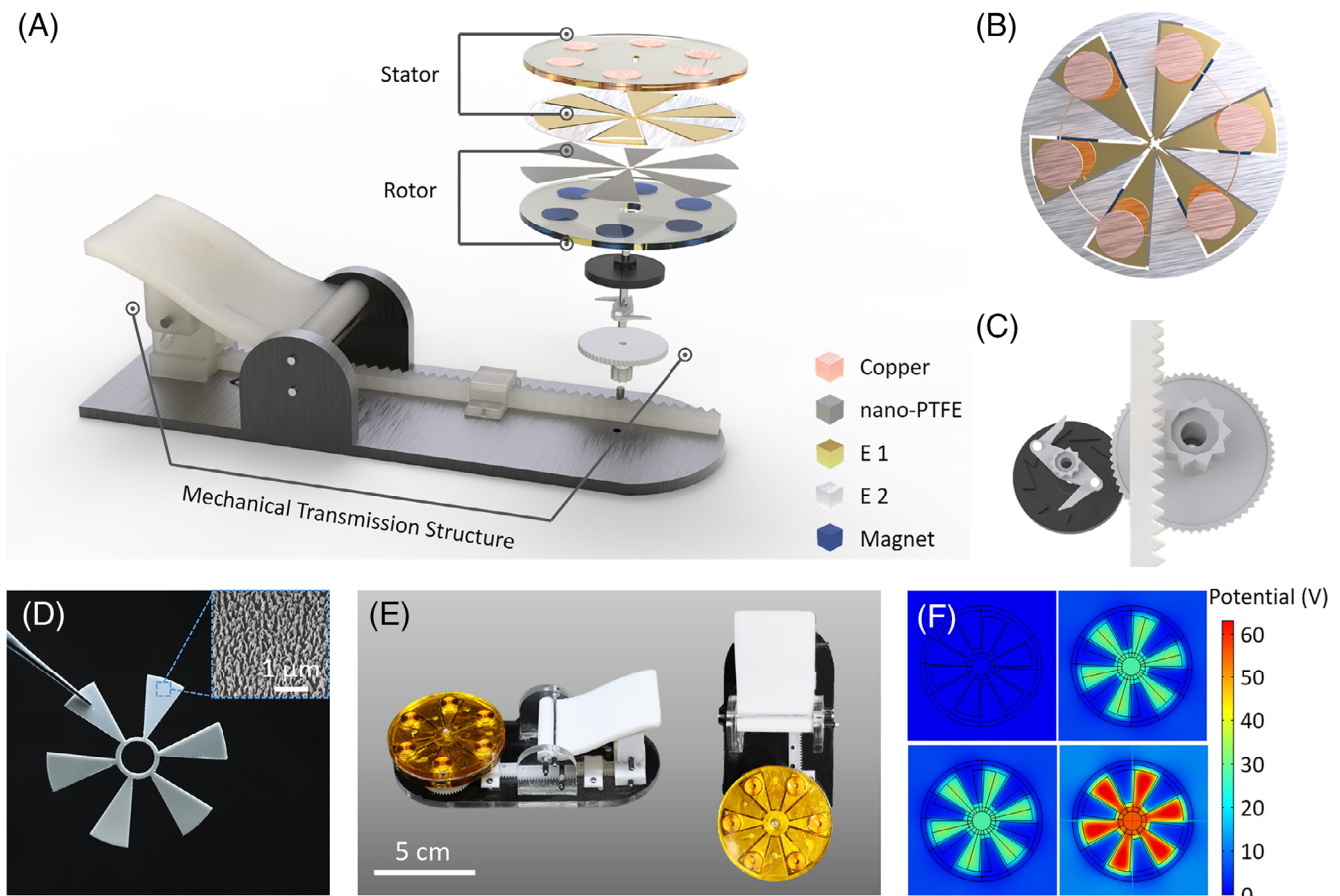


FIGURE 1 A, The schematic diagram of the basic structure of wearable noncontact free-rotating hybrid nanogenerator (WRG) composed of the hybrid nanogenerator and the wearable gravitational potential energy storage portion. B and C, The enlarged schematic of the hybrid nanogenerator and the gear transmission structure. D, Digital image of the tribo-charged layer and the scanning electron microscopic image of the nanostructure on the polytetrafluoroethylene film (scale bar: 1 μm). E, Digital image of WRG (scale bar: 5 cm). F, Simulation result of the induced potential differences between the two aluminum electrodes at the four steps of motion in a full cycle

the rotor. Then the WRG can generate an uninterrupted electric power based on electrostatic induction and electromagnetic induction. To expound the working principle of the TENG part, we calculate the potential distribution of the electrodes at different rotating motion states by utilizing the COMSOL Multiphysics software which was based on finite-element simulation (Figure 1F).

The working principle of hybrid nanogenerator is schematically described in Figure 2A–D. The hybrid nanogenerator can be divided into two parts: a TENG and an EMG. The working process of the TENG is mainly composed of the following two steps: an initial contact charging step and a cyclic rotating electrostatic induction step.^{41,42} Firstly, the tailored PTFE film is brought into contact with a piece of aluminum sheet which is referred to as electrode 1 (E1), while another complementary part of the aluminum sheet named electrode 2 (E2). In this process, the free electrons from the aluminum sheet will be injected into the surface of PTFE film, because of the different triboelectric polarities of the two materials. As a

result, a net negative charge is retained on the PTFE film surface and a net positive charge is retained on the aluminum sheet (Figure S2). The two layers were then separated with a 1-mm-thick air medium in between.

Secondly, a complete cycle of the freestanding electrostatic induction includes four steps during the rotating movement (Figure 2A).⁴³ In the initial state (step I), only a few electrons could flow from E2 to E1, because there are a relatively small distance of the vertical separation compared to the horizontal distance between the mass centers of two adjacent different metal electrodes. With the PTFE film rotating from E1 to E2, the electrons are flowing from E2 to E1 to eliminate the potential difference generated by the stable net negative charges on the PTFE film (step II). Until the PTFE sector film overlaps with E2 completely, the majority of the electrons have flowed to E1 and leaving most of the positive charges on E2 (step III). In the next stage of the movement, the analyzed part of the PTFE sector film moves toward the next segment of E1. The electrons will flow back from E2 to

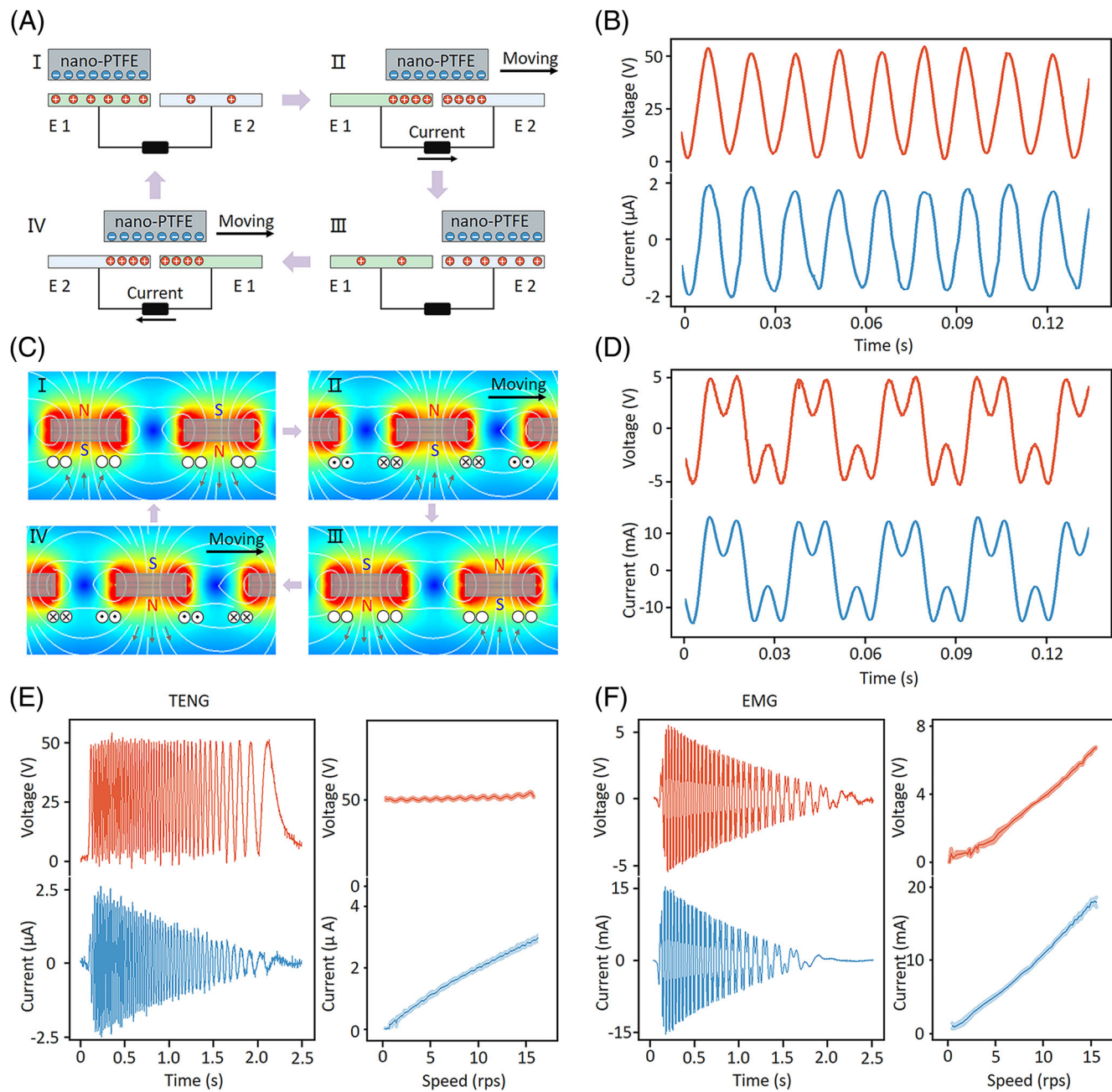


FIGURE 2 A, Schematic diagram of the working mechanism of triboelectric nanogenerator (TENG) under the relative rotation between the tribo-charged layer and metal electrodes in a complete cycle. B, The short-circuit current and open-circuit voltage of TENG at a steady speed driven by a direct current motor (about 11 rps). C, Schematic diagram of the working principle of an electromagnetic generator (EMG) under the relative rotation between the coils and the magnets in a complete cycle, where the symbols \oplus and \otimes represent the output currents that flow in and out of the plane, respectively. D, Short-circuit current and open-circuit voltage of EMG driven by the linear motor (1 Hz). E and F, The output performance of TENG and EMG under a single load press, respectively

E1, resulting in the output current with an opposite direction (step IV), until the analyzed PTFE film segments rotating back to another position like the original one. That is an operation cycle of the energy conversion of the TENG. The working principle of the EMG is based on Faraday electromagnetic induction (Figure 2C). During the circle rotation of the magnets carried by the

acrylic plate, the EMG can generate an alternating current through periodic variation of magnetic flux in coils.^{44,45}

The performance of the TENG and the EMG drove by a direct current motor (about 11 rps) is measured. The short-circuit current and the open-circuit voltage are shown in Figure 2B and D, respectively. The TENG can

produce a higher voltage output (~50 V), and the EMG produces a higher current output (~10 mA).

The linear motor was used to simulate the human body's gravitational potential energy change to test the electrical output performance of a WRG (Figure 2E,F). The single load press can drive the hybrid nanogenerator to reach a maximum rotating speed of 13.74 rps. An effective output time over two seconds can be achieved. The TENG can deliver a continuous open-circuit voltage of about 51.5 V and a short-circuit current of about 2.5 μ A. The peaks of the voltage remain stable with the gradual decrease in the rotational speed, while the short-circuit current gradually decreases. The open-circuit voltage and the short-circuit current can be derived by the equation as follows^{41,43,46}:

$$Q_{SC,final} = \int_0^l \frac{\sigma w dk}{1 + \left(\frac{C_2(k)}{C_1(k)}\right)_{x=g+l}} - \int_0^l \frac{\sigma w dk}{1 + \left(\frac{C_2(k)}{C_1(k)}\right)_{x=0}} \quad (1)$$

$$I_{SC} = \frac{dQ}{dt} \quad (2)$$

$$V_{OC} = \frac{Q}{C}. \quad (3)$$

Here, Q_{sc} is the short-circuit transferred charges. The width of the PTFE film is defined as w . We assume that only a small region of dk in the bottom dielectric surface (the distance of this region to the left edge of the bottom dielectric surface is k) contains the tribo-charges with a density of σ , and correspondingly the total charges on metal electrode 1 and 2 are $\sigma w dk$. $C_i(k)$ is the capacitance between this small surface $\sigma w dk$ and metal electrode. Thus, there is no correlation between voltage and rotating speed. The I_{SC} has a linear dependency with rotating speed.

For the EMG, the short-circuit current and the open-circuit voltage can reach up to 15 mA and 5.6 V, respectively. Both the short-circuit current and the open-circuit voltage decrease with the gradual reduction of the rotational speed. The open-circuit voltage and the short circuit current can be derived by the equation as follow⁴⁴:

$$V_{OC} = \frac{d\emptyset}{dt} \quad (4)$$

$$I_{SC} = R \frac{d\emptyset}{dt} \quad (5)$$

Here, V_{OC} is the open-circuit voltage, \emptyset refers to magnetic flux, t refers to time, R is source impedance,

and I_{SC} refers to short-circuit current. Thus, the I_{SC} has a linear dependency voltage and current with rotating speed.

The effective output of the energy harvesters is improved significantly when driven by a single load press, benefitting from the wearable gravitational potential energy storage portion. To accurately and intuitively evaluate the relationship between the electrical output performances of the WRG and the rotating speed of the rotor, the peaks of the output have been measured and analyzed in Figure 2E,F.

To drive the electronics stably and continuously, a battery and capacitor are used as the energy storage unit. The charging circuit diagram of the WRG is shown in Figure 3A. The charging capacity of the TENG, the EMG, and hybrid generator are studied systematically. Here, the WRG is driven by a linear motor. It is obvious that the charging ability of the hybrid generator is superior to the TENG and EMG (Figure 3B). In the initial stage (in the early 130 seconds) of the charging test, the EMG contributes the majority of the charging capacity of the WRG but quickly stagnate with the voltage of the capacitor close to the charging voltage of the EMG. After about 380 seconds, the charging capability of the TENG begins to exceed that of the EMG, becoming the major contributing part in the WRG because the TENG has the higher output voltage. In other words, the EMG contributes the most electrical energy in the process of turbulent charging, while the TENG mainly provides the energy of trickle charging.⁴⁷ The complementarity between the TENG and EMG improves the charging capacity of the hybrid generator. The charging capability of the WRG for the commercial lithium-ion battery (~3.4 mAh) has also been evaluated, which can be charged from 1.9 to 3.3 V in 2 minutes, as shown in Figure 3C.

To investigate the impedances of the TENG and EMG unit of the WRG, the output current and voltage are measured under the different loading resistances. With an unified 1 Hz load press, the output voltage of the EMG increases with the loading resistances increasing until 300 Ω and then turns to decrease. The maximum output power during the whole operation process is about 13.8 mW (Figure 3E). The output voltage of the TENG exhibits a noticeable increase with the loading resistance increasing, where the maximum output power of the TENG is about 40.3 μ W under a 5 M Ω loading resistance (Figure 3F).

In order to demonstrate that the WRG can be used as the power source for information electronics, it is integrated into the commercial shoes and power for a GPS (Figure 4B-E). The gravitational potential energy change of the human body caused by running and walking are

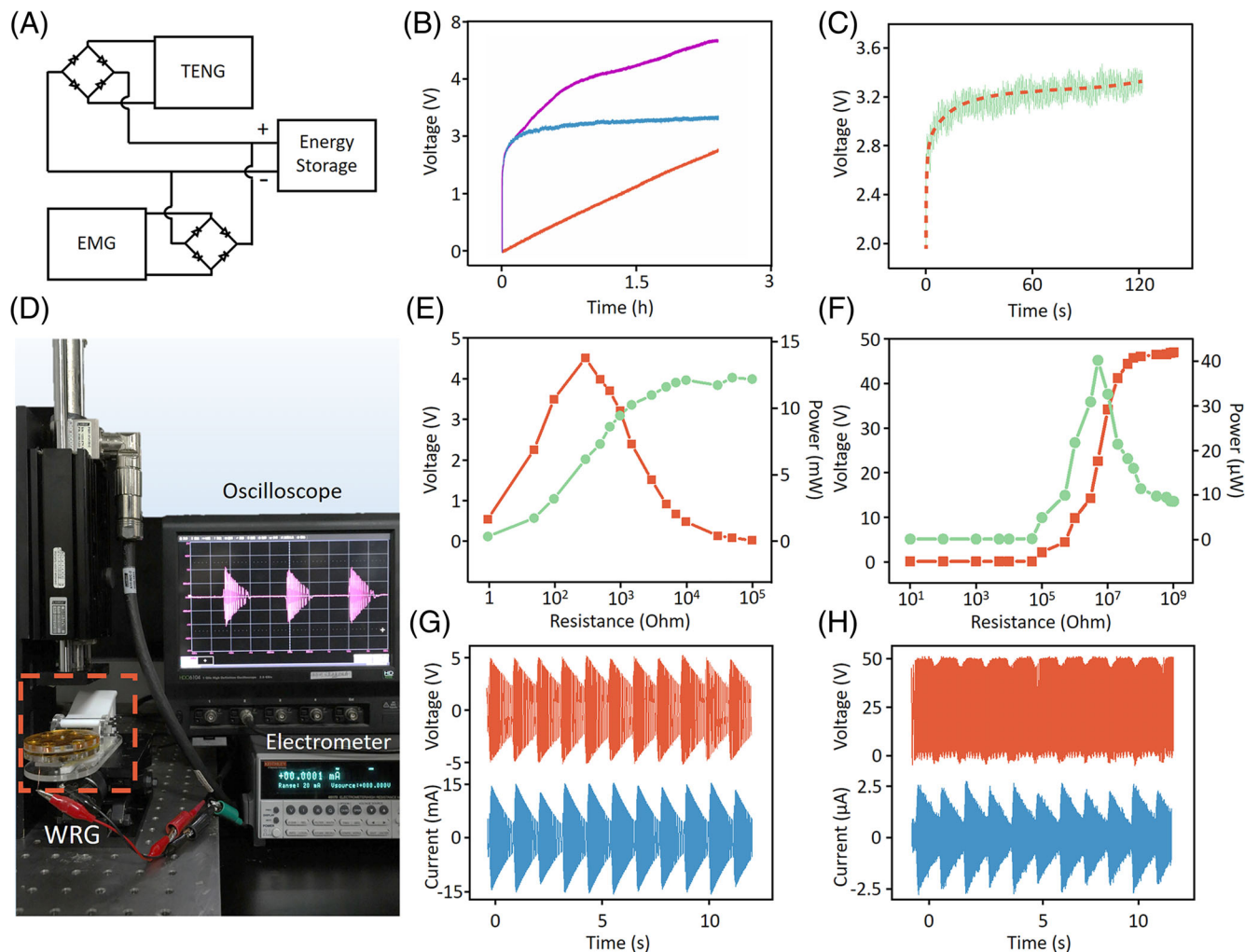


FIGURE 3 A, Circuit diagram of wearable noncontact free-rotating hybrid nanogenerator (WRG). B, Capacitor (1 mF) charge curve of each part and WRG. C, Lithium-ion battery (~3.4 mAh) charge curve of WRG. D, Schematic diagram of load press and electrical measure system for WRG. E and F, The relationships between the output voltage/power and the loading resistance of EMG (E) and triboelectric nanogenerator (TENG) (F). G and H, The continuous output voltage/current of EMG (G) and TENG (H) at a 1-Hz frequency load press

harvested to charge the battery (0.8 mAh) of the GPS. We successfully demonstrate a self-powered GPS system to monitor the location of the moving individual in real time. A route is obtained on an electronic map by the self-powered GPS system (Figure 4D), which will provide the potential applications in an emergency of the electrical energy shortage, especially in the remote areas. Figure 4E explains the charging process by the WRG and the discharging process by the GPS of a capacitor. Firstly, the capacitor (470 μ F) is charged to 3.4 V in 8 seconds and keeps being charged by the WRG. Then, with the GPS enabled, the voltage of the capacitor decreases to 2.1 V sharply and enters the standby period of 4 seconds. The WRG can charge the capacitor of the GPS to the operating voltage during this standby period, which will realize a self-powered GPS working in real time and continuously.

Furthermore, the universality of the WRG as a power source is also demonstrated. It can power the information electronics with different operating voltage and power consumption. Figure 5 G-I depicts the actual operating condition of the different electronics which are powered by the WRG. For intuitively and fully reveal the universality applications of the WRG, it is utilized to power three types of the representative information electronics, including calculator (rated voltage of 1.5 V), wireless temperature sensor (rated voltage of 3 V,) and mobile phone (rated voltage of 5 V). It is noted that the WRG can drive these devices to work continuously due to the long effective output time and high output power. By converting the human body's gravitational potential energy into the rotational kinetic energy of the rotor, the WRG can generate a relatively high effective output to power multifarious wearable/portable electronics.



FIGURE 4 Applications of wearable noncontact free-rotating hybrid nanogenerator (WRG). A, Design the technical route of WRG. WRG could be utilized in information emission, reception, and compute. B-E, Application of a self-powered GPS system based on WRG. C, Charge curve of a capacitor ($470 \mu\text{F}$) by WRG for GPS system. D, Image of the electronic map. E, Digital photograph of the self-powered GPS system. F, LEDs lighted up by WRG. G-I, Application as the universal power source for mobile phone, calculator charger, and wireless temperature sensor, respectively

3 | CONCLUSION

In summary, we have introduced a WRG that consists of the hybrid nanogenerator part and the wearable

gravitational potential energy storage part. The noncontinuous and low-frequency gravitational potential energy is converted into the continuous rotational kinetic energy by the mechanical transmission structure. This

mechanical energy storage technology can be used in wide wearable/portable applications with miniaturization.

The TENG and EMG generated power based on electrostatic induction and electromagnetic induction, which are no-contact effects with little mutual interference. Thus, they can be easily connected to the grid for power generation. The hybrid method is expected to be applied in a broad field in micro-/nano-energy and large-scale energy system.

The WRG could be integrated into the commercial shoes to harvest human-motion energy, which can provide a stable and efficient power source for information electronics. The output power can meet the most of the information electronics with different operation voltage (1-5 V) and power consumption (0.1-10 mA), such as GPS, calculator, wireless temperature sensor, and even mobile phone. Furthermore, it is expected to build the next generation of self-powered wearable/portable information electronics in the future.

4 | METHODS

4.0.1 | Characterization methods

The scanning electron microscopic image is taken by the Hitachi field emission scanning electron microscope (SU 8020). The output voltage and current of the WRG are measured by an electrometer (Keithley 6517 System) and recorded by an oscilloscope (Teledyne LeCroy HD 4096), and the mechanical excitation is provided by a linear motor (LinMot PS01-37*120-C).

4.0.2 | Calculation of the peak power

Peak power (PP) is employed to evaluate the output performance of the WRG. PP can be derived by the equation as follows:

$$PP = V_{max} \times I_{max}. \quad (6)$$

Here, V_{max} is the maximum output voltage. I_{max} is the maximum output current at different load resistance.

4.0.3 | Fabrication of tribo-charged layer

The nanostructure of the PTFE film is fabricated by the ICP etching system (SENTECH/SI 500). Firstly, a piece of the PTFE film ($\sim 300 \mu\text{m}$ in thickness) is tailored into a six-segment structure and rinsed by alcohol and deionized water. The Au (Aurum) is sputtered onto the

PTFE film surface about 30 seconds and fabricated as the mask for the etching process. After that, this tailored PTFE film is etched by ICP reactive ion etching for 300 seconds (ICP power: 400 and 100 W, respectively). The reaction gases in the ICP process are CF_4 (30.0 sccm), Ar (15.0 sccm), and O_2 (10.0 sccm). Then, the Au bottom electrode (50 nm) is deposited on the PTFE film surface by magnetron sputter (Denton Discovery 635) for 15 minutes (sputter power 100 W). Finally, the Au bottom electrode is connected by a wire to ground, and a polarization voltage of 5 kV is applied through the corona needle for 15 minutes.

ACKNOWLEDGMENTS

The authors acknowledges funding from National Key R&D Project from Minister of Science and Technology, China (2016YFA0202703, 2016YFC1102202), National Natural Science Foundation of China (61875015, 11421202, 81971770 and 21801019), National Postdoctoral Program for Innovative Talent (BX20190026), China Postdoctoral Science Foundation (2019M660410), the Beijing Natural Science Foundation (7204275), the 111 Project (B13003), and the National Youth Talent Support Program.

CONFLICT OF INTEREST

The authors declare no conflict of interest.

AUTHOR CONTRIBUTIONS

D.J., H.O., and B.S. contributed equally to this work. Z. Li, Y.F., D.J., H.O., B.S. conceived the project. D.J., H.O., B.S., P.T., and Y.Z. carried out WRG fabrication and electrical characteristic work. D.J., C.Z., and X.Q., accomplish the material characterization. S.C. and Y.X. carried out the finite-element simulation of WRG. D.J., and H.O. have processed the data and carried out the statistical analysis of the electrical signal. All authors discussed and co-wrote the paper. The authors declare that they have no competing interests.

DATA AVAILABILITY STATEMENT

All data needed to evaluate the conclusions in the paper are present in the paper and/or the Supporting Information. Additional data related to this paper may be requested from the authors.

ORCID

Zhou Li  <https://orcid.org/0000-0002-9952-7296>

REFERENCES

1. Wang L, Tang H, Cierny M. Device-to-device link admission policy based on social interaction information. *IEEE T Veh Technol.* 2015;64(9):4180-4186.

2. Zhu ML, Shi QF, He T, et al. Self-powered and self-functional cotton sock using piezoelectric and triboelectric hybrid mechanism for healthcare and sports monitoring. *ACS Nano*. 2019;13(2):1940-1952.
3. Guan H, Zhong T, He H, et al. A self-powered wearable sweat-evaporation-biosensing analyzer for building sports big data. *Nano Energy*. 2019;59:754-761.
4. Ouyang H, Tian JJ, Sun GL, et al. Self-powered pulse sensor for antidiastole of cardiovascular disease. *Adv Mater*. 2017;29(40):1703456.
5. Cheng XL, Meng B, Zhang XS, et al. Wearable electrode-free triboelectric generator for harvesting biomechanical energy. *Nano Energy*. 2015;12:19-25.
6. Donelan JM, Li Q, Naing V, Hoffer JA, Weber DJ, Kuo AD. Biomechanical energy harvesting: generating electricity during walking with minimal user effort. *Science*. 2008;319(5864):807-810.
7. He T, Wang H, Wang J, et al. Self-sustainable wearable textile nano-energy nano-system (NENS) for next-generation healthcare applications. *Adv Sci*. 2019;6(24):1901437.
8. Park DY, Joe DJ, Kim DH, et al. Self-powered real-time arterial pulse monitoring using ultrathin epidermal piezoelectric sensors. *Adv Mater*. 2017;29(37):1702308.
9. Chen XX, Song Y, Su ZM, et al. Flexible fiber-based hybrid nanogenerator for biomechanical energy harvesting and physiological monitoring. *Nano Energy*. 2017;38:43-50.
10. Yoon HJ, Ryu H, Kim SW. Sustainable powering triboelectric nanogenerators: approaches and the path towards efficient use. *Nano Energy*. 2018;51:270-285.
11. Wang X, Wang ZL, Yang Y. Hybridized nanogenerator for simultaneously scavenging mechanical and thermal energies by electromagnetic-triboelectric-thermoelectric effects. *Nano Energy*. 2016;26:164-171.
12. Wang ZL. Triboelectric Nanogenerators as new energy Technology for Self-Powered Systems and as active mechanical and chemical sensors. *ACS Nano*. 2013;7(11):9533-9557.
13. Ryu H, Yoon HJ, Kim SW. Hybrid energy harvesters: toward sustainable energy harvesting. *Adv Mater*. 2019;31(34):1802898.
14. Guo HY, Yeh MH, Lai YC, et al. All-in-one shape-adaptive self-charging power package for wearable electronics. *ACS Nano*. 2016;10(11):10580-10588.
15. Cui NY, Liu JM, Gu L, Bai S, Chen X, Qin Y. Wearable Triboelectric generator for powering the portable electronic devices. *ACS Appl Mater Inter*. 2015;7(33):18225-18230.
16. Zhong T, Zhang M, Fu Y, et al. An artificial triboelectricity-brain-behavior closed loop for intelligent olfactory substitution. *Nano Energy*. 2019;63:103884.
17. Wang ZL, Song JH. Piezoelectric nanogenerators based on zinc oxide nanowire arrays. *Science*. 2006;312(5771):242-246.
18. Fan FR, Tian ZQ, Wang ZL. Flexible triboelectric generator! *Nano Energy*. 2012;1(2):328-334.
19. Yang PK, Lin L, Yi F, et al. A flexible, stretchable and shape-adaptive approach for versatile energy conversion and self-powered biomedical monitoring. *Adv Mater*. 2015;27(25):3817-3824.
20. Yu YH, Li ZD, Wang YM, Gong S, Wang X. Sequential infiltration synthesis of doped polymer films with tunable electrical properties for efficient Triboelectric Nanogenerator development. *Adv Mater*. 2015;27(33):4938-4944.
21. Lee SH, Jeong CK, Hwang GT, Lee KJ. Self-powered flexible inorganic electronic system. *Nano Energy*. 2015;14:111-125.
22. Ouyang H, Li Z. The first technology can compete with piezoelectricity to harvest ultrasound energy for powering medical implants. *Sci Bull*. 2019;64(21):1565-1566.
23. Hinchet R, Yoon HJ, Ryu H, et al. Transcutaneous ultrasound energy harvesting using capacitive triboelectric technology. *Science*. 2019;365(6452):491-494.
24. Hou TC, Yang Y, Zhang H, et al. Triboelectric nanogenerator built inside shoe insole for harvesting walking energy. *Nano Energy*. 2013;2(5):856-862.
25. Zhu G, Bai P, Chen J, Wang ZL. Power-generating shoe insole based on triboelectric nanogenerators for self-powered consumer electronics. *Nano Energy*. 2013;2(5):688-692.
26. Shenck NS, Paradiso JA. Energy scavenging with shoe-mounted piezoelectrics. *IEEE Micro*. 2001;21(3):30-42.
27. Hwang BU, Lee JH, Trung TQ, et al. Transparent stretchable self-powered patchable sensor platform with ultrasensitive recognition of human activities. *ACS Nano*. 2015;9(9):8801-8810.
28. Wang SH, Xie YN, Niu SM, Lin L, Wang ZL. Freestanding Triboelectric-layer-based nanogenerators for harvesting energy from a moving object or human motion in contact and non-contact modes. *Adv Mater*. 2014;26(18):2818-2824.
29. Shi BJ, Liu Z, Zheng Q, et al. Body-integrated self-powered system for wearable and implantable applications. *ACS Nano*. 2019;13(5):6017-6024.
30. Zou Y, Tan PC, Shi BJ, et al. A bionic stretchable nanogenerator for underwater sensing and energy harvesting. *Nat Commun*. 2019;10:2695.
31. Sun J, Yang A, Zhao C, Liu F, Li Z. Recent progress of nanogenerators acting as biomedical sensors in vivo. *Sci Bull*. 2019;64(18):1336-1347.
32. Chen T, Shi Q, Zhu M, et al. Triboelectric self-powered wearable flexible patch as 3D motion control interface for robotic manipulator. *ACS Nano*. 2018;12(11):11561-11571.
33. Shi Q, Zhang Z, Chen T, Lee C. Minimalist and multi-functional human machine interface (HMI) using a flexible wearable triboelectric patch. *Nano Energy*. 2019;62:355-366.
34. Hou C, Chen T, Li YF, et al. A rotational pendulum based electromagnetic/triboelectric hybrid-generator for ultra-low-frequency vibrations aiming at human motion and blue energy applications. *Nano Energy*. 2019;63:103871.
35. Kuang SY, Chen J, Cheng XB, Zhu G, Wang ZL. Two-dimensional rotary triboelectric nanogenerator as a portable and wearable power source for electronics. *Nano Energy*. 2015;17:10-16.
36. Xie YN, Wang SH, Niu SM, et al. Multi-layered disk triboelectric nanogenerator for harvesting hydropower. *Nano Energy*. 2014;6:129-136.
37. Kishor N, Saini RP, Singh SP. A review on hydropower plant models and control. *Renew Sustain Energy Rev*. 2007;11(5):776-796.
38. Swider DJ. Compressed air energy storage in an electricity system with significant wind power generation. *IEEE T Energy Convers*. 2007;22(1):95-102.
39. Hu YR. HuaW, will the symbiotic pacemaker, a self-powered cardiac implanted electronic device, be the next evolution in pacemaker technology? *Sci Bull*. 2019;64(13):877-878.

40. Zhao LM, Zheng Q, Ouyang H, et al. A size-unlimited surface microstructure modification method for achieving high performance triboelectric nanogenerator. *Nano Energy*. 2016;28:172-178.
41. Niu SM, Liu Y, Chen XY, et al. Theory of freestanding triboelectric-layer-based nanogenerators. *Nano Energy*. 2015;12:760-774.
42. Lin L, Wang SH, Niu SM, Liu C, Xie YN, Wang ZL. Noncontact free-rotating disk triboelectric nanogenerator as a sustainable energy harvester and self-powered mechanical sensor. *ACS Appl Mater Inter*. 2014;6(4):3031-3038.
43. Wang ZL. On Maxwell's displacement current for energy and sensors: the origin of nanogenerators. *Mater Today*. 2017;20(2):74-82.
44. Zhang C, Tang W, Han CB, Fan FR, Wang ZL. Theoretical comparison, equivalent transformation, and conjunction operations of electromagnetic induction generator and Triboelectric Nanogenerator for harvesting mechanical energy. *Adv Mater*. 2014;26(22):3580-3591.
45. Zhong XD, Yang Y, Wang X, Wang ZL. Rotating-disk-based hybridized electromagnetic-triboelectric nanogenerator for scavenging biomechanical energy as a mobile power source. *Nano Energy*. 2015;13:771-780.
46. Wang ZL, Lin L, Chen J, Niu S, Zi Y. *Triboelectric Nanogenerators*. Switzerland: Springer; 2016.
47. Tan PC, Zheng Q, Zou Y, et al. A battery-like self-charge universal module for motional energy harvest. *Adv Energy Mater*. 2019;9(36):1901875.

SUPPORTING INFORMATION

Additional supporting information may be found online in the Supporting Information section at the end of this article.

How to cite this article: Jiang D, Ouyang H, Shi B, et al. A wearable noncontact free-rotating hybrid nanogenerator for self-powered electronics. *InfoMat*. 2020;2:1191–1200. <https://doi.org/10.1002/inf2.12103>